ORIGINAL RESEARCH

Derivation and Validation of a Nomogram to Predict In-Hospital Complications in Children with Tetralogy of Fallot Repaired at an Older Age

Hong Liu, MD, PhD;* Si-qiang Zheng, MD, PhD;* Xin-ya Li, MD, PhD;* Zhi-hua Zeng, MD, PhD;* Ji-sheng Zhong, MD;* Jun-quan Chen, MD;* Tao Chen, MD;* Zhi-gang Liu, MD, PhD; Xiao-cheng Liu, MD; Yong-feng Shao, MD, PhD

***Background*—**We aimed to develop and validate a prediction model for in-hospital complications in children with tetralogy of Fallot repaired at an older age.

***Methods and Results*—**A total of 513 pediatric patients from the Tianjin data set formed a derivation cohort, and 158 pediatric patients from the Hefei and Xiamen data sets formed validation cohorts. We applied least absolute shrinkage and selection operator analysis for variable selection and logistic regression coefficients for risk scoring. We classified patients into different risk categorizations by threshold analysis and investigated the association with in-hospital complications using logistic regression. In-hospital complications were defined as death, need for extensive pharmacologic support (vasoactive-inotrope score of ≥20), and need for mechanical circulatory support. We developed a nomogram based on risk classifier and independent baseline variables using a multivariable logistic model. Based on risk scores weighted by 11 preoperative and 4 intraoperative selected variables, we classified patients as low, intermediate, and high risk in the derivation cohort. With reference to the low-risk group, the intermediate- and high-risk groups conferred significantly higher in-hospital complication risks (adjusted odds ratio: 2.721 [95% CI, 1.267–5.841], P=0.0102; 9.297 [95% CI, 4.601–18.786], P<0.0001). A nomogram integrating the ARIAR-Risk classifier (absolute and relative low risk, intermediate risk, and aggressive and refractory high risk) with age and mean blood pressure showed good discrimination and goodness-of-fit for derivation (area under the receiver operating characteristic curve: 0.785 [95% CI, 0.731–0.839]; Hosmer-Lemeshow test, P=0.544) and external validation (area under the receiver operating characteristic curve: 0.759 [95% CI, 0.636–0.881]; Hosmer-Lemeshow test, P=0.508).

***Conclusions*—**A risk-classifier–oriented nomogram is a reliable prediction model for in-hospital complications in children with tetralogy of Fallot repaired at an older age, and strengthens risk/benefit–based decision-making. **(*J Am Heart Assoc*. 2019;8: e013388. DOI: 10.1161/JAHA.119.013388.)**

Key Words: low cardiac output syndrome • nomogram • tetralogy of Fallot

Tetralogy of Fallot is the most common cyanotic congenital heart defect globally and carries high morbidity and mortality risk if not treated immediately and properly.[1–3] However, infants and children who have undergone surgical repair with cardiopulmonary bypass (CPB) are at high risk for significant morbidity and mortality.[4–6] Although these potential adverse outcomes have been well described, a critical need remains to develop a predictive model by integrating

From the Department of Cardiovascular Surgery, TEDA International Cardiovascular Hospital, Chinese Academy of Medical Sciences & Peking Union Medical College, Tianjin, China (H.L., S.-q.Z., Z.-h.Z., J.-q.C., T.C., Z.-g.L., X.-c.L.); Department of Cardiovascular Surgery, First Hospital of Nanjing Medical University, Nanjing, China (H.L., Y.-f.S.); Department of Cardiovascular Surgery, the First Hospital of University of Science and Technology of China, Hefei, China (X.-y.L.); Department of Cardiovascular Surgery, Xiamen Cardiovascular Hospital, Xiamen University, Xiamen, China (J.-s.Z.).

Accompanying Tables S1 through S4 and Figures S1 through S4 are available at https://www.ahajournals.org/doi/suppl/10.1161/JAHA.119.013388

*Dr Liu, Dr Zheng, Dr Li, Dr Zeng, Dr Zhong, Dr Jun-quan Chen, and Dr Tao Chen contributed equally to this work.

Correspondence to: Yong-feng Shao, MD, PhD, Department of Cardiovascular Surgery, the First Hospital of Nanjing Medical University, Nanjing, China. E-mail: yfshaojph@sina.com; and Zhi-gang Liu, MD, PhD, or Hong Liu, MD, PhD, Department of Cardiovascular Surgery, TEDA International Cardiovascular Hospital, Chinese Academy of Medical Sciences & Peking Union Medical College, Tianjin, China. E-mails: liuzgtich@sina.com and dr.hongliu@foxmail.com

Received May 24, 2019; accepted September 19, 2019.

Clinical Perspective

What Is New?

- We developed a nomogram model integrating the ARIAR-Risk classifier (absolute and relative low risk, intermediate risk, and aggressive and refractory high risk) with age at surgery and mean blood pressure to predict in-hospital complications after tetralogy of Fallot repair and further validated models in both derivation and validation cohorts, suggesting good discrimination and goodness-of-fit.

What Are the Clinical Implications?

- A risk-classifier–oriented nomogram is a reliable prognostic tool for the assessment of in-hospital complications in children with tetralogy of Fallot repaired at an older age and is easy to implement in clinical practice.

baseline, clinical, and procedural factors that are indicative of illness severity and short-term outcome. The identification of these variables could aid in appropriate risk stratification, monitoring, and clinical management for the treatment of tetralogy of Fallot.[7,8]

Various models have been developed to predict postoperative mortality and morbidity in cardiac surgery.[9,10] In contrast, no predictive models combine baseline, clinical, and procedural factors to predict poor outcomes after tetralogy of Fallot repair, given the heterogeneities of congenital heart diseases.[11,12]

We performed a study incorporating pre- and intraoperative characteristics with the aim of identifying and validating a risk classifier that predicts in-hospital complications in Chinese children with tetralogy of Fallot repaired at an older age defined as over 6 months-1 year. Moreover, we integrated risk-classifier and independent baseline predictors to generate a nomogram, backed by internal and external validation, to advance clinical evaluation for patient therapeutics and to strengthen risk/benefit–based decision-making.

Methods

Data Availability

The data, analytic methods, and study materials will not be made available to other researchers for purposes of reproducing the results or replicating the procedure. Because this study uses data from human subjects, the data and everything pertaining to them are governed by the TedaICH Data Protection Agency and can only be made available to additional researchers if a formal request is filed with the TedaICH authorities.

Study Design and Participants

Between January 1, 2012, and July 31, 2018, 513 consecutive pediatric patients with tetralogy of Fallot at Teda International Cardiovascular Hospital (Tianjin, China) formed the derivation cohort. We used an independent data set of 158 pediatric patients (validation cohort) from Anhui Provincial Hospital (Hefei, China) between January 1, 2004, to July 31, 2018, and Xiamen Cardiovascular Hospital (Xiamen, China) between January 1, 2012, to July 31, 2018, to externally validate this model (Figure S1). We included pediatric patients aged 10 days to 18 years who underwent complete repair of tetralogy of Fallot with CPB. Both derivation and validation cohorts included only tetralogy of Fallot patients, excluding those with pulmonary atresia with ventricular septal defect or double-outlet right ventricle. Ethics and regulatory approval for the study was obtained from each local ethics committee. Written informed consent was obtained from each patient before surgery.

Candidate Predictors

Consistent data for each patient were collected from the medical records, and all candidate predictors were selected on the basis of detailed literature reviews and clinical evidence within the confines of data availability. Baseline characteristics included continuous and categorized age at surgery,[13] sex, weight, height, body mass index, heart rate, respiratory rate, systolic and diastolic blood pressure, blood pressure difference, and mean arterial pressure. The clinical profiles included Tet spell history, systemic arterial saturation, cyanosis degree, right bundle-branch block, New York Heart Association (NYHA) class (modified Ross scoring for infants[14]), and hematocrit. Anatomic profiles included ventricular septal defect subtypes, defect scale (the ratio of the defect to aortic root diameter), overriding aorta, predominantly interventricular shunting, right ventricular outflow tract (RVOT) pressure gradient, RVOT obstruction level, McGoon index, left ventricular (LV) ejection fraction, indexed left atrial diameter, indexed right atrial diameter, indexed LV end-diastolic diameter, indexed RV end-diastolic diameter, indexed LV end-diastolic volume, collateral arteries, and patent ductus arteriosus. Surgical profiles included repair approach, RVOT obstruction repair, transannular patch, pulmonary patch, and tricuspid valve detachment. Extracorporeal profiles included cannulation approach, reoxygenation level, cardioplegia, and CPB temperature and duration. These detailed and specific definitions are listed in Table S1.

Study Outcomes

The primary clinical end point was in-hospital complications, including death, need for extensive pharmacologic

cardiovascular support (highest vasoactive-inotropic score of >20 points), and need for additional mechanical circulatory support within the first 72 hours after operation, whichever occurred first. Vasoactive-inotrope score was calculated daily as per Gaies et al,[15] where vasoactive-inotrope score=dopamine dose (lg/kg per minute)+dobutamine dose (lg/kg per 9 minute)+[100 × epinephrine dose (lg/kg per minute)]+[10 x milrinone dose (lg/kg per minute)]+[10 000 × vasopressin dose (U/kg per minute)]+[100 × norepinephrine dose (lg/kg per minute)]. All outcomes were adjudicated independently by an event collaborative team.

Statistical Analysis

Before data analysis, predictor variables in the derivation and validation cohorts were inspected for missing values. Among the predictors, the proportion of missing data ranged from 0 to 31.7%. To include these data from the analyses, we imputed missing data by multiple imputations by chained equations, using the *mice* package for R, in which predictive mean matching is embedded with the cases (k)=5 default. Patients with missing outcome measures and lost demographic and surgical records were excluded from both the derivation cohort (28/573, 4.9%) and the validation cohort (47/262, 17.9%; Figure S1).

Data are presented as frequencies (percentages) for categorical variables and medians (interquartile ranges [IQRs]) for continuous variables. Differences between groups were assessed using the χ^2 test or Fisher exact test for categorical variables and the Student *t* test or the Mann–Whitney *U* test for continuous variables. The pre- and postimputation data sets were compared with the Kruskal–Wallis equality-of-populations rank test for the derivation and validation cohorts.

Model derivation was performed according to Transparent Reporting of a Multivariable Prediction Model for Individual Prognosis or Diagnosis (TRIPOD) guidance.[16] We included a set of predefined prediction variables of preoperative variables comprising clinical and anatomical profiles and intraoperative variables comprising surgical and extracorporeal profiles (Tables S1 and S2). We applied least absolute shrinkage and selection operator (LASSO) analysis in a penalized logistic regression model (R package *glmnet*) to select the most useful prediction variables from all pre- and intraoperative candidates in the derivation cohort.[17] Subsequently, we constructed the prediction scoring model by assigning each patient a risk score for in-hospital complications based on the product of the expression levels for the variables selected by the LASSO analysis and the respective regression coefficients weighted by logistic regression analysis in the derivation cohort. Then we fitted the dose–response relationship between the risk score and in-hospital complications–related morbidity using generalized additive models and further found the optimal cutoff point using Empowerstats software (X&Y Solutions). The thresholds for the scores that were output from the predictive model that was used to classify patients into different risk categories were defined as the scores that gave the largest log-likelihood value in a 2-piecewise regression model.[18] The Dunnett method was used for multiple comparisons of in-hospital complication rates against a control group (lowest risk category).

We further assessed the association of risk categorizations with in-hospital complications using logistic regression for baseline characteristics. We also performed tests for linear trend by entering the median value of each category of risk score as a continuous variable in this model. We developed a in-hospital complications nomogram starting from a multivariable logistic regression model that allowed us to obtain in-hospital complications probability estimates. We included a set of predefined predictor variables of the risk-classifier and baseline characteristics (age group at surgery, sex, weight, height, body mass index, heart rate, respiratory rate, systolic blood pressure, diastolic blood pressure, pulse pressure difference, and mean arterial pressure)[19] and applied a stepwise procedure based on the Akaike information criterion (AIC) for variable selection and a multifractional polynomial for variable selection.[20]

We carried out internal validation of the model development process using a bootstrap resampling process (1000 bootstrap samples per model) to provide an unbiased estimate of model performance. To assess the external validity of model performance, using an independent and external data set of 158 pediatric patients (Hefei and Xiamen cohorts), we examined the overall accuracy (Nagelkerke's R^2), calibration (calibration plots and Hosmer–Lemeshow calibration test) and discrimination (area under receiver operating characteristic curve [AUC]).[21–23] We also plotted decision curves to assess the net benefit of nomogram-assisted decisions.[24] To investigate the cumulative incidence of in-hospital complications by age at surgery, we used Kaplan–Meier estimates with age as the time scale.[25]

To investigate whether the predictive strength of nomogram covariates would change by varying the year of surgery, we extracted the linear predictor from the nomogram and investigated the interaction between such linear predictors and the year of surgery with the Wald test.[26] We considered a 2-sided *P* value of <0.05 to be statistically significant. We performed the statistical analyses using Stata v14 (StataCorp) and R software (v3.2.0; R Foundation for Statistical Computing).

Results

The derivation cohort consisted of 513 patients who had complete surgery, with a median age of 30.7 months (IQR: 13.5–60.8 months) and 221 (43.1%) female patients. The

Table 1. Selected Baseline and Perioperative Variables of Development and Validation Cohorts After Imputation

Variables	Derivation Cohort (n=513)	Validation Cohort (n=158)	*P* Value
Baseline variables			
Age at surgery, mo	30.7 (13.5–60.8)	28.7 (13.4–55.1)	0.664
Age group at surgery, %			0.429
Infant (<1 y)	216 (42.1)	66 (41.8)	
Toddler and preschool (2–5 y)	190 (37.0)	64 (40.5)	
School-aged child (6–12 y)	92 (17.9)	21 (13.3)	
Adolescent (13–18 y)	15 (2.9)	7 (4.4)	
Mean BP, mm Hg	47.33 (42.67–50.67)	46.8 (42.1–49.3)	0.484
Preoperative variables			
Hematocrit, %	43.6 (38.1–50.5)	43.2 (38.1–49.5)	0.797
Indexed LVEDV, mL/m^2	27.1 (20.7–35.7)	27.5 (21.9–37.3)	0.364
Indexed RA diameter, mm/m^2	49.7 (40.9–56.2)	49.1 (39.5–55.6)	0.593
Cyanosis degree, %			0.902
None	137 (26.7)	45 (28.5)	
Minor	174 (33.9)	53 (33.5)	
Major	202 (39.4)	60 (38.0)	
Tet spell history, %			0.932
Absence	300 (58.5)	93 (58.9)	
Presence	213 (41.5)	65 (41.1)	
NYHA functional class, %			0.575
I–II	479 (93.4)	150 (94.94)	
III–IV	34 (6.6)	8 (5.1)	
Right bundle-branch block, %			0.567
Absence	463 (90.3)	145 (91.8)	
Presence	50 (9.8)	13 (8.2)	
Interventricular shunting, %			0.807
Predominantly left to right	58 (11.3)	17 (10.7)	
Predominantly bidirectional	432 (84.2)	132 (83.5)	
Predominantly right to left	23 (4.5)	9 (5.7)	
Aortic overriding, %			0.305
≤50%	438 (85.4)	140 (88.6)	
>50%	75 (14.6)	18 (11.4)	
McGoon index, %			0.731
>1.5	353 (68.8)	111 (70.3)	
≤1.5	160 (31.2)	47 (29.8)	
Collateral circulation, %			0.367
Minimal	383 (74.7)	109 (69.0)	
Minor	73 (14.2)	27 (17.1)	
Major	57 (11.1)	22 (13.9)	
Intraoperative variables			
Reoxygenation level, %			0.086

Continued

Table 1. Continued

Variables	Derivation Cohort (n=513)	Validation Cohort (n=158)	*P* Value
Lower (≤250 mm Hg)	262 (51.1)	93 (58.9)	
Higher (>250 mm Hg)	251 (48.9)	65 (41.1)	
Tricuspid valve detachment, %			0.858
Absence	409 (79.7)	127 (80.4)	
Presence	104 (20.3)	31 (19.6)	
RVOTO repair options, %			0.821
Parietal muscle resection	23 (4.5)	8 (5.1)	
Infundibular outflow patch	76 (14.8)	19 (12.0)	
Valve-sparing repair	130 (25.3)	43 (27.2)	
Transannular patch	284 (55.4)	88 (55.7)	
CPB duration, min	121 (90–156)	122 (95–154)	0.786
Postoperative outcome			
In-hospital complications, %	76 (14.8)	22 (13.9)	0.782
Postoperative inotropic score, point	9.00 (6.00–13.50)	8.70 (6.00–12.43)	0.256
Risk score, point	−2.097 (−2.558 to 1.581)	−2.158 (−2.647 to 1.647)	0.403

Continuous data are presented as median (interquartile range), and dichotomous data are presented as n (%). BP indicates blood pressure; CPB, cardiopulmonary bypass; LVEDV, left ventricle end-diastolic volume; NYHA, New York Heart Association; RA, right atrial; RVOTO, right ventricular outflow tract obstruction.

validation cohort consisted of 158 patients, with a median age of 28.7 months (IQR: 13.4–55.1 months) and 73 (46.2%) female patients. The occurrence of in-hospital complications was 14.8% (76/513) in the derivation cohort and 13.9% (22/158) in the validation cohort, without a significant difference between cohorts (P=0.782).

Baseline clinical and surgical characteristics after imputation in the derivation and validation cohorts are listed in Table 1 and Tables S2 and S3. Based on LASSO analysis, we identified a composite panel that consisted of 11 preoperative and 4 intraoperative variables associated with in-hospital complication morbidity in the derivation cohort, with the optimal λ penalty (AUC=0.785; Table 1; Figure 1). A risk score was calculated for each patient using a formula derived from the expression levels of these 15 variables weighted by their regression coefficients:Risk score=−2.88745+(−0.15197×cyanosis: minor)+(0.36081×−cyanosis: major)+(−0.13475×Tet spell history: absence)+(−0.53315×NYHA class: grades I–II)+(−0.23192×right bundle-branch block: absence)+(0.02408×prehematocrit: %)+(−0.00824×indexed LV end-diastolic volume: mm/m^2)+(0.00357×indexed right atrial diameter: mm/m^2)+(−0.06019×interventricular shunting: bidirectional)+(−0.17454×overriding aorta: ≤50-%)+(−0.13612×McGoon index: >1.5)+(0.04306×collaterals: major)+(−0.25836×RVOT obstruction repair: infundibular outflow patch)+(−0.00103×tricuspid valve detachment: absence)+(−0.25053×reoxygenation level: lower)+(0.00769×CPB duration: minute).

A dose dependency of in-hospital complications risk was identified for increasing risk score (odds ratio [OR]: 4.243 [95% CI, 2.881–6.247], P<0.0001; Figure 2A, Figure S2A). Patients with in-hospital complications had a significantly higher risk score than those without in-hospital complications (median: −1.300 [IQR: −2.059 to 0.944] versus −2.196 [IQR: −2.643 to 1.714], P<0.001; Figure S2B). Based on threshold analysis, we generated 2 cutoff values of −2.1488 and −1.5957 to classify such scores into *low risk* (−2.149 or fewer points), *intermediate risk* (−2.149 to −1.596 points), and *high risk* (−1.596 or more points) for the probability of in-hospital complications in the derivation cohort. Subsequently, triple-risk (ie, low, intermediate, high) categories were further subdivided into the following subcategories based on threshold analysis of subgroups (Figure 2A): *absolute* low risk (−2.816 or fewer points), *relative* low risk (−2.816 to −2.149), intermediate risk (−2.149 to −1.596), *aggressive* high risk (−1.596 to −0.813), and *refractory* high risk (−0.813 or more points) subcategories (ARIAR-Risk classifier). Before multivariable adjustment, both the triple-risk classifier and the ARIAR-Risk classifier showed a strong independent predictive factor for in-hospital complications in the derivation cohort (Figure S3A and S3B). After multivariable adjustment for baseline characteristics, with reference to the low-risk group, the intermediate- and high-risk groups conferred significantly higher risk of in-hospital complications in the derivation cohort (adjusted OR: 2.721 [95% CI, 1.267–

5.841], *P*=0.0102; 9.297 [95% CI, 4.601–18.786], *P*<0.0001, respectively; Figure 2B). Similarly, with reference to the intermediate-risk group, the low-risk groups conferred significantly lower risk of in-hospital complications (adjusted OR: 0.092 [95% CI, 0.018–0.716] for absolute low risk; 0.486 [95% CI, 0.222–1.066] for relative low risk), and the high-risk groups conferred a significantly higher risk of in-hospital complications (adjusted OR: 2.701 [95% CI, 1.373–5.316] for aggressive high risk; 8.442 [95% CI, 3.191–22.336] for refractory high risk; Figure 2C). We performed multiple comparisons for ARIAR-Risk categories and triple-risk categories, and the results are summarized in Table S4. The AUC comparison showed that the ARIAR-Risk classifier exhibited prediction performance superior to the triple-risk classifier (AUC: 0.753 [95% CI, 0.697–0.809] versus 0.733 [95% CI, 0.675–0.791]; *P*=0.0014) in predicting in-hospital complications (Figure 3). Consequently, the ARIAR-Risk classifier was selected as the major variable instead of the triple-risk classifier to develop the nomogram model.

In addition to the ARIAR-Risk classifier, AIC-based stepwise-selected variables (patient age group and mean blood pressure) on the multivariable logistic model had a significant effect on in-hospital complications (all Wald tests *P*<0.05) in the derivation cohort: age group at surgery (infant [referent]; toddler and preschool, AUC: 0.502 [95% CI, 0.265–0.952]; school age child, AUC: 0.871 [95% CI, 0.413–1.837]; adolescent, AUC: 1.619 [95% CI, 0.417–6.285]) and mean blood pressure (per mm Hg, OR: 0.974 [95% CI, 0.948–1.001]). Based on the ARIAR-Risk classifier and the independent risk factors selected, we developed a nomogram using a multivariable logistic model to predict the probability of in-hospital complications after surgery for a patient (Figure 4A) based on the AIC-selected logistic model: 0.19653−0.68956×(age group: toddler and preschool)−0.13795×(age group: school age child)+0.48166×(age group: adolescent)−0.02633×mean blood pressure (mm Hg)−2.30699×(ARIAR-Risk: absolute low risk)−0.76712×(ARIAR-Risk: relative low risk)+1.02621×(ARIAR-Risk: aggressive high risk)+2.09761×(ARIAR-Risk: refractory high risk).

In addition, we further developed another nomogram by integrating the ARIAR-Risk classifier and multifractional polynomial–selected variables (patient age group and mean blood pressure divided by 100). We compared multifractional polynomial–selected and AIC-selected nomogram models and found that the 2 models had similar prediction performance in terms of AUC (multifractional polynomial–selected model, AUC: 0.785 [95% CI, 0.730–0.839]; AIC-selected model, AUC: 0.785 [95% CI, 0.731–0.839]), so we finally selected the AIC-based nomogram model for validation, taking into consideration the clinical significance, in which there is no need for mean blood pressure divided by 100.

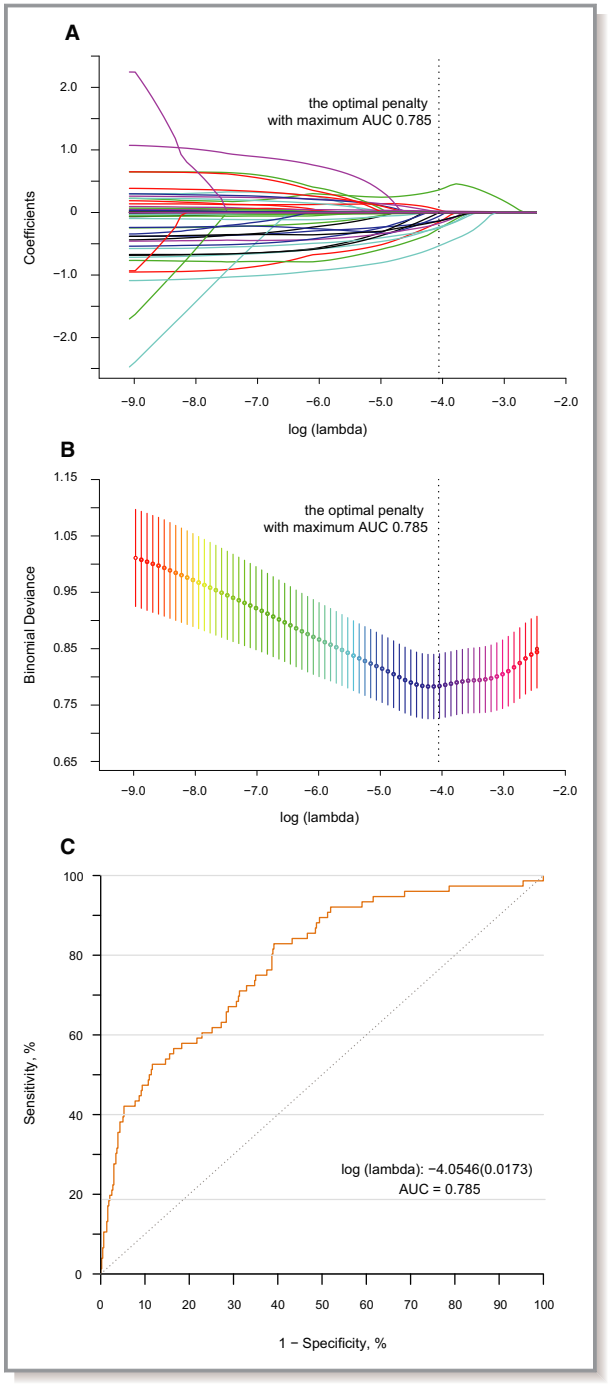

Figure 1. LASSO model profile plots. **A**, Coefficient profile plots showing how size of the coefficients of preoperative and intraoperative factors shrinks with increasing value of the λ penalty, with the factors and their regression coefficients selected for the model based on the optimal λ for the LASSO model. **B**, Penalty plot for the LASSO model; color error bars indicate standard error. **C**, The optimal λ penalty of the LASSO model with a maximum AUC of 0.785. AUC indicates area under the receiver operating characteristic curve; LASSO, least absolute shrinkage and selection operator.

The overall accuracy of the in-hospital complications nomogram was moderate for the derivation cohort (Nagelkerke's R^2=0.206) and for the validation cohort (Nagelkerke's

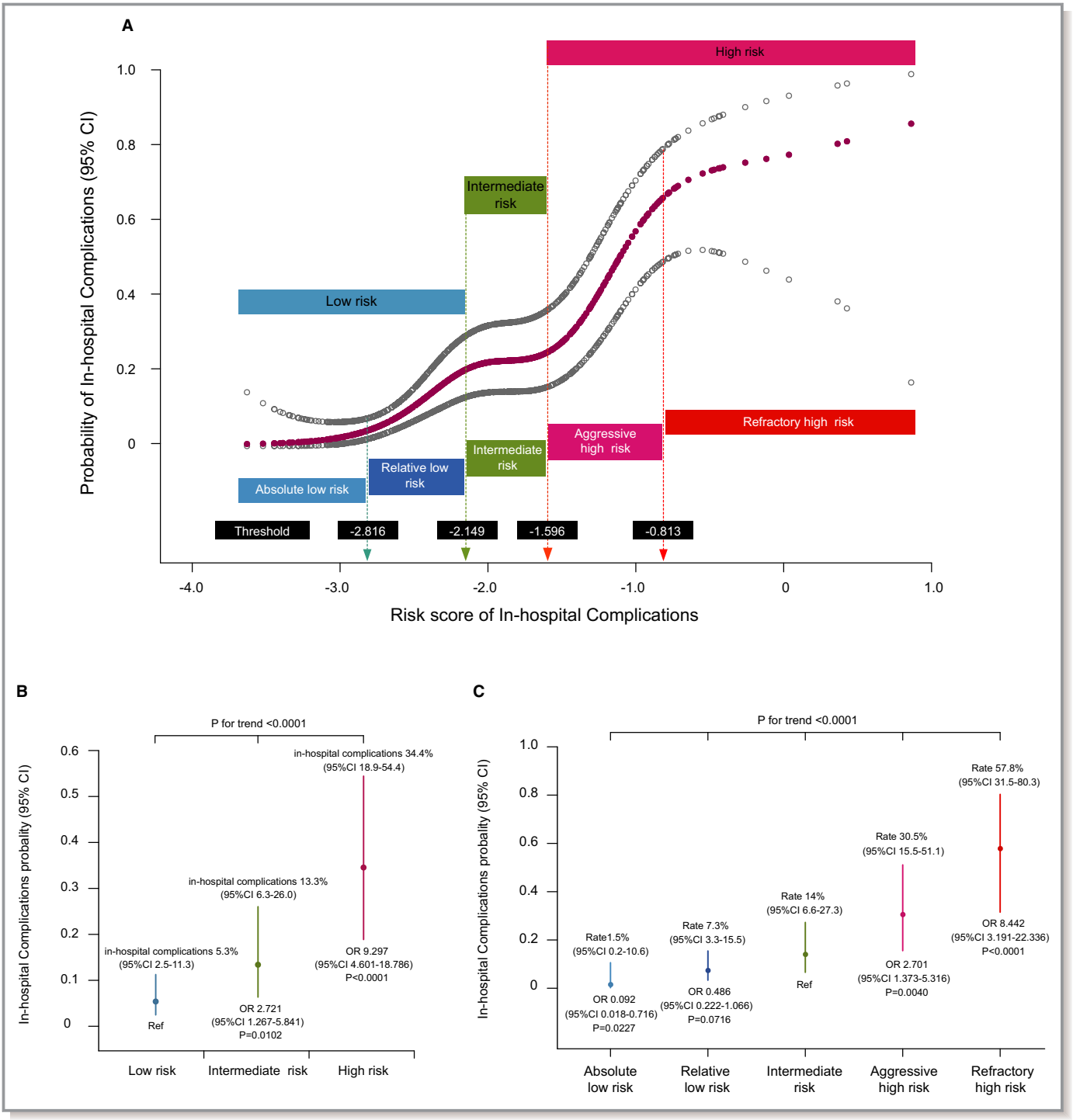

Figure 2. Risk-based classifier profiles in a derivation cohort. **A**, Dose-response relationship between risk score and morbidity from in-hospital complications and threshold points for classifying patients into risk categorizations. **B** and **C**, Adjusted association between the triple-risk (ie, low, intermediate, high) classifier (**B**) and the ARIAR-Risk classifier (**C**) and probability and OR of in-hospital complications with 95% CIs. ARIAR-Risk indicates absolute and relative low risk, intermediate risk, and aggressive and refractory high risk; OR, odds ratio.

R^2=0.298). The discrimination of the nomogram was moderate to good at most for the derivation cohort (AUC: 0.785 [95% CI, 0.731–0.839]), for internal validation with bootstrapping (AUC: 0.784 [95% CI, 0.729–0.837]), and for the external validation cohort (AUC: 0.759 [95% CI, 0.636–0.881]; Figure 4B–4D). The specificity and sensitivity were 0.7735 and 0.7105, respectively, for the derivation cohort; 0.7231 and 0.7500, respectively, for internal validation with

bootstrapping; and 0.8382 and 0.6500, respectively, for the external validation cohort (Table 2).

The calibration plots of the nomogram for in-hospital complication probability showed moderate to good performance at most (Figure 4E–4G). The Hosmer–Lemeshow calibration test was not significant both for the derivation cohort (χ^2=6.933, P=0.544) and the external validation cohort (χ^2=7.264, P=0.508); both indicate a good fit. The decision curves for in-hospital complication probability in the derivation cohort, internal validation with bootstrapping, and external validation cohort (Figure 4H–4J) showed relatively good performance for the model in terms of clinical application. If the threshold probability in clinical decision was more than 10%, then use of the nomogram model to detect in-hospital complications showed a greater advantage than assuming that all patients would develop in-hospital complications or that no patients would develop in-hospital complications.

Figure 5A through 5C shows the cumulative probability of in-hospital complications by age at surgery and how this probability depends on the overall, triple-risk, and ARIAR-Risk classifiers. Patients with high risk scores had the highest cumulative incidence, whereas intermediate- and low-risk patients had significantly lesser cumulative risk patterns (both P for log-rank <0.0001). As observed with the nomogram model, no significant change was detected for the prognostic strength of in-hospital complication predictors by varying the year of surgery (Wald test for interaction: mean arterial pressure×year of surgery, P=0.563), even if the ARIAR-Risk classifier and age group at surgery were modeled as continuous scales (risk score×year of surgery, P=0.568; age at surgery×year of surgery, P=0.374; Figure S4A–S4C).

Given the heterogeneity of age, we divided the derivation cohort into 2 subgroups (406 younger and 107 older patients) based on the age threshold of 60 months to investigate whether the nomogram model performed equally well in older and younger patients. The discrimination of the nomogram was better for the younger subgroup (AUC: 0.791 [95% CI, 0.734–0.849]) than the older subgroup (AUC: 0.759 [95% CI, 0.700–0.819]). The Hosmer–Lemeshow calibration test was not significant for either the younger subgroup (χ^2=3.215, P=0.920) or the older subgroup (χ^2=8.713, P=0.367). The accuracy of this model was moderate for the younger subgroup (Nagelkerke's R^2=0.225) and older subgroup (Nagelkerke's R^2=0.163).

Discussion

In this multicenter retrospective cohort study, we developed and validated a novel predictive tool based on 11 preoperative and 4 intraoperative variables selected to improve the ability to predict in-hospital complications in Chinese children with tetralogy of Fallot repaired at an older age. Our results showed that the triple-risk classifier developed in this study categorized patients into low-, intermediate-, and high-risk groups of patients who had significantly different probabilities of in-hospital complications. Furthermore, the optimized ARIAR-Risk classifier showed significantly better predictive performance than the triple-risk classifier at predicting in-hospital complications in tetralogy of Fallot repaired at an older age. We built a nomogram based on the ARIAR-Risk classifier and independent baseline variables to predict individual risk of in-hospital complications, and it showed good discrimination and goodness-of-fit.

Given that tetralogy of Fallot is a heterogeneous disease and in-hospital complications result from multifactorial synergies,[1,4] exploring the key determinants involving initiation and derivation of in-hospital complications might help to improve prognostic and therapeutic strategies.[7,8,27] In the current study, we identified a panel of 15 perioperative variables that effectively predict in-hospital complications in children with tetralogy of Fallot repaired at an older age. Among these candidates, the presence of a lower McGoon ratio, right-to-left shunting, lower indexed LV end-diastolic volume, right bundle-branch block, and major aortopulmonary collaterals were previously shown to be associated with more severe RVOT obstruction and thus to contribute to worse outcome.[28] In patients with preexisting major cyanosis, Tet spell history, higher hematocrit, and inferior NYHA class, the cardiac autoregulatory capacity is

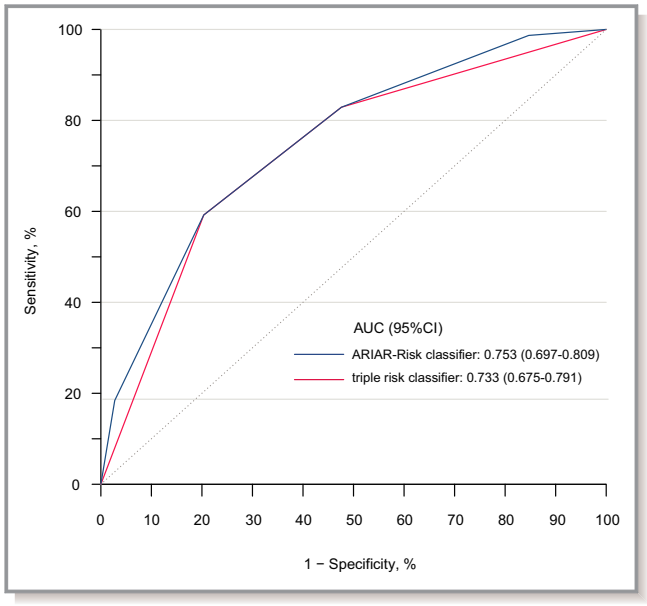

Figure 3. Comparison of the ARIAR-Risk classifier and the triple-risk (ie, low, intermediate, high) classifier. AUC indicates area under the receiver operating characteristic curve. ARIAR-Risk indicates absolute and relative low risk, intermediate risk, and aggressive and refractory high risk.

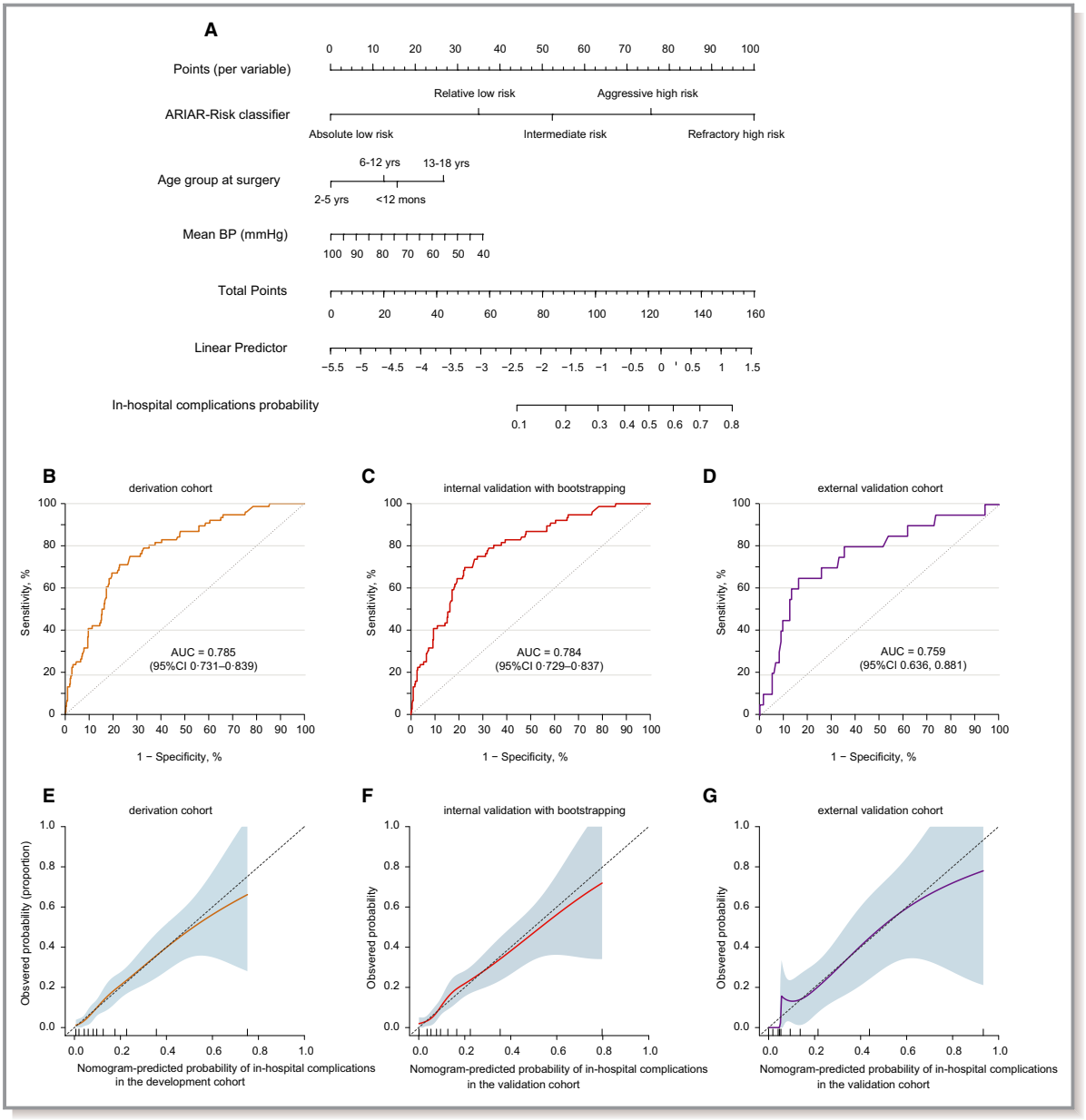

Figure 4. Derivation and validation of an in-hospital complications nomogram. **A**, In-hospital complications nomogram. This nomogram provides a method to calculate the probability of cumulative incidence of developing postoperative in-hospital complications after complete repair of tetralogy of Fallot, on the basis of a patient's combination of covariates. AUCs for the derivation cohort (**B**), internal validation with bootstrapping (**C**), and external validation cohort (**D**) of the in-hospital complications nomogram. Calibration plots for the derivation cohort (**E**), internal validation with bootstrapping (**F**), and external validation cohort (**G**) of the in-hospital complications nomogram. Shaded area is 95% CIs of the cumulative incidence. Dashed line is the reference line, which would indicate where an ideal nomogram would lie. Decision curves for the in-hospital complications nomogram in the derivation cohort (**H**), internal validation with bootstrapping (**I**), and external validation cohort (**J**). Gray solid line indicates net benefit of a strategy of treating all patients. Blue dotted line indicates net benefit of treating no patients. Color solid line indicates net benefit of a strategy of treating patients for the derivation cohort, for internal validation with bootstrapping, and for the external validation cohort according to the nomogram predictions. AUC indicates area under the receiver operating characteristic curve; BP, blood pressure.

likely impaired, thus rendering heart more susceptible to surgical strikes with bypass and compromising functional recovery.[8]

Interestingly, our results showed that higher overriding is associated with increased risk of in-hospital complications; this finding could be explained by the fact that patients with

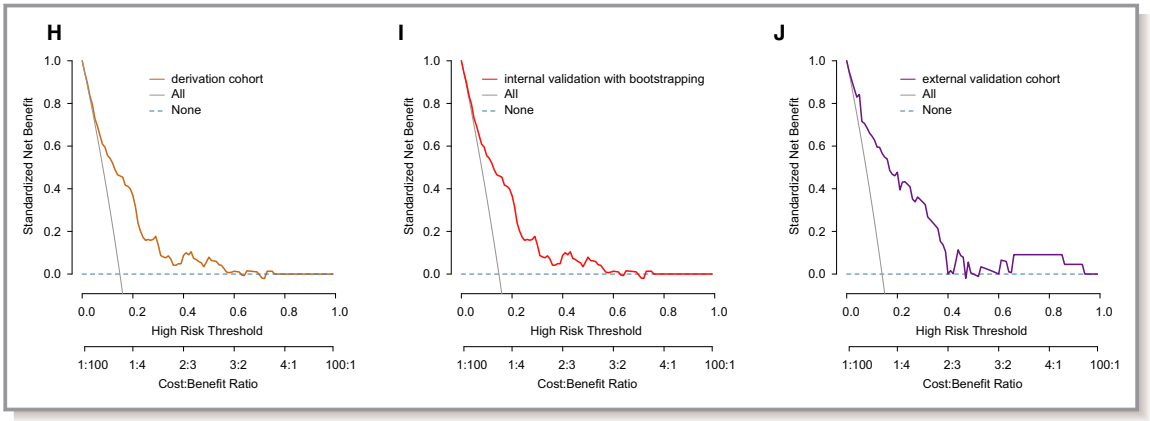

Figure 4. Continued

higher overriding frequently require larger Dacron patches to close ventricular septal defect areas, resulting in myocardial deformations and geometric impairments.[29,30] Isolated infundibular outflow patch,[31] absence of tricuspid valve detachment, and shorter CPB duration were found to relate to less invasive strikes, which result in better preservation of cardiac structural integrity and minimization of systemic inflammatory responses mainly induced by ischemia/reperfusion injury. Clinically promising results have been achieved by lowering reoxygenation via adjusting oxygen pressure during bypass in patients with cyanotic heart diseases; this approach likely alleviated hypoxia/reoxygenation injury to reduce the risk of major organ dysfunctions in cyanotic patients.[32,33] Consequently, this prediction model may help clinicians identify high-risk patients following repaired tetralogy of Fallot.

Although some risk factors and biomarkers have been associated with in-hospital complications following pediatric cardiac surgery,[12,34] this specific nomogram is still lacking for prediction of the risk of in-hospital complications for an individual, especially for repaired tetralogy of Fallot; therefore, we incorporated the ARIAR-Risk classifier. This classifier provides insights into pathophysiologic, anatomic, and procedural heterogeneities of tetralogy of Fallot repair and independent baseline variables that reflect sociodemographic and baseline clinical heterogeneities to develop a nomogram for predicting in-hospital complications. This nomogram was further verified in external validation cohorts and exhibited good model performance; it might provide a simple and accurate method for predicting prognoses in pediatric patients with repaired tetralogy of Fallot.[7,8,35]

Apart from 15 clinical, anatomic–physiologic, and procedural candidates, we identified age at surgery as an independent predictor of in-hospital complications. Our analysis demonstrated an increasing trend for in-hospital complications with increasing age and decreasing mean blood pressure. Baseline lower mean blood pressure is indicative of reduced blood supply to organs and end-organ damage, such as the brain and the heart, which leads to serious consequences.[36] Three months to 3 to 4 years is a good age at which to operate on tetralogy of Fallot in clinical practice; however, the median patient was approximately 5 years of age in our study. Five is relatively old for repair in much of the world, where most cases are repaired in infancy or shortly thereafter because older age is associated with a stiffer right ventricle, higher diastolic dysfunction, and increased chance of mortality and morbidity due to prolonged cyanosis.[37] Given the heterogeneity of age, we divided the derivation cohort into younger and older subgroups to

Table 2. Performances of Nomogram for Derivation Cohort, Internal Validation With Bootstrapping, and External Validation Cohort

	Derivation Cohort	Internal Validation With Bootstrapping	External Validation Cohort
Specificity	0.774	0.723	0.838
Sensitivity	0.711	0.750	0.650
Accuracy	0.764	0.727	0.814
Positive likelihood ratio	3.136	2.709	4.018
Negative likelihood ratio	0.374	0.346	0.418
Positive predictive value	0.353	0.320	0.371
Negative predictive value	0.939	0.943	0.942

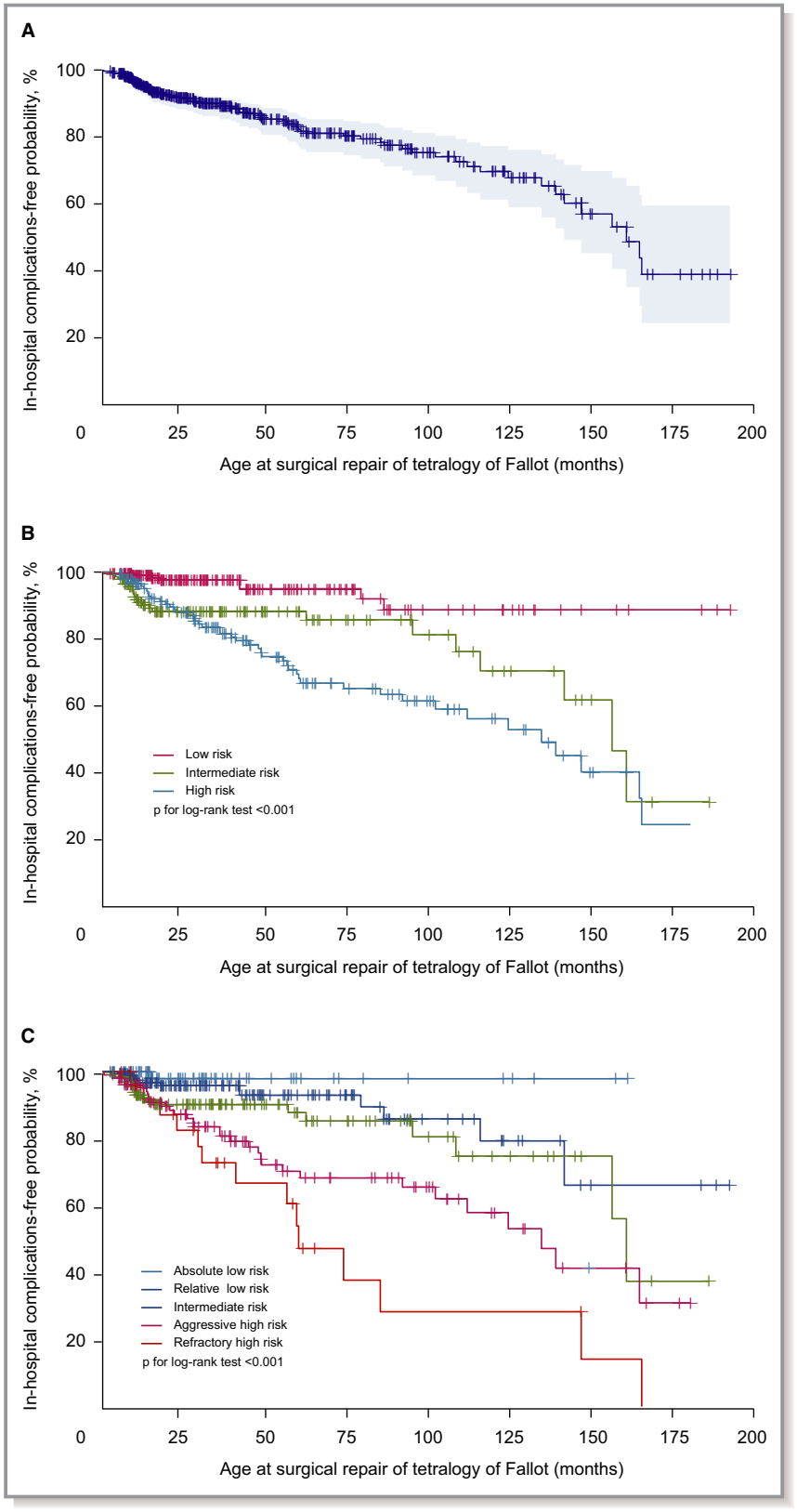

Figure 5. Cumulative risks of in-hospital complications with increasing age at surgery. Kaplan–Meier curves by overall (**A**), triple-risk (ie, low, intermediate, high) classifier (**B**), and ARIAR-Risk classifier (**C**). Shaded area is 95% CIs of the cumulative incidence.

investigate whether the nomogram model performed equally well in older and younger patients. Our results suggested that the discrimination of the nomogram model was better for the younger subgroup than for the older subgroup. Taking into consideration the sample cohort age, the generalizability of our results must be interpreted in the context of demographic and clinical characteristics, especially for age at surgery in our current study.

Our findings should be interpreted in the context of the study's limitations. First, surgical strategy selection in the study was determined by balancing the risks and benefits associated with each procedure in conjunction with the available baseline factors and the preferences of cardiac surgeons involved; therefore, the specific expertise may differ from those of other practitioners, potentially limiting the generalizability of these results to other institutions. In addition, although our sample size of 513 patients in the derivation set was small compared with established prediction tools based on large numbers of congenital heart disease patients, the power of a study is driven by the number of events, not simply by the total number of patients. With a prevalence of ≈15% of patients who developed in-hospital complications in our derivation cohort, the size of our study was adequate to power the derivation of risk prediction models. In addition, some missing data were imputed, limiting the generalizability of the study, especially with validation in a small cohort; prospective large-scale studies are needed to further verify the current findings.

Conclusions

To the best of our knowledge, this study is the first to incorporate per- and intraoperative characteristics to develop and validate a predictive model for in-hospital complications in children with tetralogy of Fallot repaired at an older age. Our findings show that the triple-risk classifier can effectively classify patients into different risk groups of in-hospital complications, thereby improving predictive value for the assessment of patient prognosis. Moreover, we showed that the optimized ARIAR-Risk classifier might have significantly better predictive performance than the triple-risk classifier for identifying patients who would develop in-hospital complications following tetralogy of Fallot repair at an older age. A nomogram including the ARIAR-Risk classifier might help clinicians in directing personalized therapeutic regimen selection for patients with tetralogy of Fallot repaired at an older age. However, attention should be paid to the fact that the patients included in this study underwent surgical repair of tetralogy of Fallot at an older age that is different from much of the rest of the world.

Acknowledgments

We thank Xiao-qing Chen, MD, PhD, for her important reference for article revision.

Sources of Funding

This work was mainly supported by the Fundamental Research Funds for the Central Universities (No. 3332018189) and National Clinical Key Specialty Construction Projects of China.

Disclosures

None.

References

1. Pitz C, Webb GD, Redington AN. Tetralogy of Fallot. *Lancet*. 2009;374:1462–1471.
2. Murphy JG, Gersh BJ, Mair DD, Fuster V, McGoon MD, Ilstrup DM, McGoon DC, Kirklin JW, Danielson GK. Long-term outcome in patients undergoing surgical repair of tetralogy of Fallot. *N Engl J Med*. 1993;329:593–599.
3. Chiu SN, Wang JK, Chen HC, Lin MT, Wu ET, Chen CA, Huang SC, Chang CI, Chen YS, Chiu IS, Chen CL, Wu MH. Long-term survival and unnatural deaths of patients with repaired tetralogy of Fallot in an Asian cohort. *Circ Cardiovasc Qual Outcomes*. 2012;5:120–125.
4. Al Habib HF, Jacobs JP, Mavroudis C, Tchervenkov CI, O'Brien SM, Mohammadi S, Jacobs ML. Contemporary patterns of management of tetralogy of Fallot: data from the Society of Thoracic Surgeons database. *Ann Thorac Surg*. 2010;90:813–819.
5. Epting CL, McBride ME, Wald EL, Costello JM. Pathophysiology of post-operative low cardiac output syndrome. *Curr Vasc Pharmacol*. 2016;14:14–23.
6. Anderson RH, Spicer DE, Giroud JM, Mohun TJ. Tetralogy of Fallot: nosological, morphological, and morphogenetic considerations. *Cardiol Young*. 2013;23:858–866.
7. Dickerson HA, Cabrera AG. General pre-operative and post-operative considerations in pediatric cardiac patients. In: Da Cruz E, Ivy D, Jaggers J, eds. *Pediatric and Congenital Cardiology*. London: Cardiac Surgery and Intensive Care. Springer; 2014:117–130.
8. Downing TE, Kim YY. Tetralogy of Fallot: general principles of management. *Cardiol Clin*. 2015;33:531–541.
9. Ettema RG, Peelen LM, Schuurmans MJ, Nierich AP, Kalkman CJ, Moons KG. Prediction models for prolonged intensive care stay after cardiac surgery: systematic review and validation study. *Circulation*. 2010;122:682–689.
10. Granton J, Cheng D. Risk stratifcation models for cardiac surgery. *Semin Cardiothorac Vasc Anesth*. 2008;12:167–174.
11. Chowdhury UK, Sathia S, Ray R, Singh R, Pradeep KK, Venugopal P. Histopathology of the right ventricular outflow tract and its relationship to clinical outcomes and arrhythmias in patients with tetralogy of Fallot. *J Thorac Cardiovasc Surg*. 2006;132:270–277.
12. Norgård G, Gatzoulis MA, Moraes F, Lincoln C, Shore DF, Shinebourne EA, Redington AN. Relationship between type of outflow tract repair and postoperative right ventricular diastolic physiology in tetralogy of Fallot. *Implications for long-term outcome. Circulation*. 1996;94:3276–3280.
13. Goldstein B, Giroir B, Randolph A; International Consensus Conference on Pediatric Sepsis. International pediatric sepsis consensus conference: definitions for sepsis and organ dysfunction in pediatrics. *Pediatr Crit Care Med*. 2005;6:2–8.
14. Ross RD, Bollinger RO, Pinsky WW. Grading the severity of congestive heart failure in infants. *Pediatr Cardiol*. 1992;13:72–75.
15. Gaies MG, Jeffries HE, Niebler RA, Pasquali SK, Donohue JE, Yu S, Gall C, Rice TB, Thiagarajan RR. Vasoactive-inotropic score is associated with outcome after infant cardiac surgery: an analysis from the Pediatric Cardiac Critical Care Consortium and Virtual PICU System Registries. *Pediatr Crit Care Med*. 2014;15:529–537.

16. Collins GS, Reitsma JB, Altman DG, Moons KG. Transparent reporting of a multivariable prediction model for individual prognosis or diagnosis (TRIPOD): the TRIPOD statement. *BMJ*. 2015;350:g7594.
17. Tibshirani RJ. Regression shrinkage and selection via the LASSO. *J R Stat Soc B*. 1996;58:267–288.
18. Piepho HP, Ogutu JO. Inference for the break point in segmented regression with application to longitudinal data. *Biometrical J*. 2003;45:591–601.
19. Durrleman S, Simon R. Flexible regression models with cubic splines. *Stat Med*. 1989;8:551–561.
20. Akaike H. Information theory as an extension of the maximum likelihood principle. In: Petrov BN, Csaki F, eds. *Second International Symposium on Information Theory*. Budapest: Akademiai Kiado; 1973:267–281.
21. Harrell FE Jr, Lee KL, Mark DB. Multivariable prognostic models: issues in developing models, evaluating assumptions and adequacy, and measuring and reducing errors. *Stat Med*. 1996;15:361–387.
22. Alba AC, Agoritsas T, Walsh M, Hanna S, Iorio A, Devereaux PJ, McGinn T, Guyatt G. Discrimination and calibration of clinical prediction models: users' guides to the medical literature. *JAMA*. 2017;318:1377–1384.
23. Hosmer DW, Hosmer T, Le Cessie S, Lemeshow S. A comparison of goodness-of-fit tests for the logistic regression model. *Stat Med*. 1997;16:965–980.
24. Vickers AJ, Elkin EB. Decision curve analysis: a novel method for evaluating prediction models. *Med Decis Making*. 2006;26:565–574.
25. Qizilbash N, Gregson J, Johnson ME, Pearce N, Douglas I, Wing K, Evans SJW, Pocock SJ. BMI and risk of dementia in two million people over two decades: a retrospective cohort study. *Lancet Diabetes Endocrinol*. 2015;3:431–436.
26. Callegaro D, Miceli R, Bonvalot S, Ferguson P, Strauss DC, Levy A, Griffin A, Hayes AJ, Stacchiotti S, Pechoux CL, Smith MJ, Fiore M, Dei Tos AP, Smith HG, Mariani L, Wunder JS, Pollock RE, Casali PG, Gronchi A. Derivation and external validation of two nomograms to predict overall survival and occurrence of distant metastases in adults after surgical resection of localised soft-tissue sarcomas of the extremities: a retrospective analysis. *Lancet Oncol*. 2016;17:671–680.
27. Wessel DL. Managing low cardiac output syndrome after congenital heart surgery. *Crit Care Med*. 2001;29:S220–S230.
28. Valente AM, Cook S, Festa P, Ko HH, Krishnamurthy R, Taylor AM, Warnes CA, Kreutzer J, Geva T. Multimodality imaging guidelines for patients with repaired tetralogy of Fallot: a report from the American Society of Echocardiography: developed in collaboration with the Society for Cardiovascular Magnetic Resonance and the Society for Pediatric Radiology. *J Am Soc Echocardiogr*. 2014;27:111–141.
29. Zhong L, Gobeawan L, Su Y, Tan JL, Ghista D, Chua T, Tan RS, Kassab G. Right ventricular regional wall curvedness and area strain in patients with repaired tetralogy of Fallot. *Am J Physiol Heart Circ Physiol*. 2012;302:H1306–H1316.
30. Orwat S, Diller GP, Kempny A, Radke R, Peters B, Kühne T, Boethig D, Gutberlet M, Dubowy KO, Beerbaum P, Sarikouch S, Baumgartner H; German Competence Network for Congenital Heart Defects Investigators. Myocardial deformation parameters predict outcome in patients with repaired tetralogy of Fallot. *Heart*. 2016;102:209–215.
31. Uebing A, Gibson DG, Babu-Narayan SV, Diller GP, Dimopoulos K, Goktekin O, Spence MS, Andersen K, Henein MY, Gatzoulis MA, Li W. Right ventricular mechanics and QRS duration in patients with repaired tetralogy of Fallot: implications of infundibular disease. *Circulation*. 2007;116:1532–1539.
32. Ghorbel MT, Mokhtari A, Sheikh M, Angelini GD, Caputo M. Controlled reoxygenation cardiopulmonary bypass is associated with reduced transcriptomic changes in cyanotic tetralogy of Fallot patients undergoing surgery. *Physiol Genomics*. 2012;44:1098–1106.
33. Babu B, Bhat S, Prabuswamy HP, Kamalapurkar G, Kumar HV, Libu GK, Shilpa S, Lokesh BK. Controlling oxygenation during initiation of cardiopulmonary bypass: can it improve immediate postoperative outcomes in cyanotic children undergoing cardiac surgery? A prospective randomized study. *World J Pediatr Congenit Heart Surg*. 2017;3:310–316.
34. Pérez-Navero JL, de la Torre-Aguilar MJ, Ibarra de la Rosa I, Gil-Campos M, Gómez-Guzmán E, Merino-Cejas C, Muñoz-Villanueva MC, Llorente-Cantarero FJ. Cardiac biomarkers of low cardiac output syndrome in the postoperative period after congenital heart disease surgery in children. *Rev Esp Cardiol (Engl Ed)*. 2017;70:267–274.
35. Oualha M, Urien S, Spreux-Varoquaux O, Bordessoule A, D'Agostino I, Pouard P, Tréluyer JM. Pharmacokinetics, hemodynamic and metabolic effects of epinephrine to prevent post-operative low cardiac output syndrome in children. *Crit Care*. 2014;18:R23.
36. Sembiring K, Ramayani OR, Lubis M. Mean blood pressure difference among adolescents based on dyssomnia types. *Open Access Maced J Med Sci*. 2018;6:293–296.
37. Bove T, François K, De Wolf D. New insights into the surgical management of tetralogy of Fallot: physiological fundamentals and clinical relevance. *Curr Pediatr Rev*. 2015;11:72–86.

Supplemental Material

Table S1. Definition of preoperative and Intraoperative variables in derivation cohort.

Variables	Method of assessment and grading	Ref.
Sociodemographic characteristics		
Age on continuous scale	Assessed at surgery	in units of month
Age at surgery as categorical scale	Pediatric age groups according to International pediatric sepsis consensus conference: Definitions for sepsis and organ dysfunction in pediatrics [1] Infant (1mon-1yr) Toddler and preschool (2-5 yrs) School age child (6-12 yrs) Adolescent (13-18 yrs)	infants vs toddler and preschool vs school age child vs adolescent
Sex	Female male	female vs male
Height	Assessed at surgery	in units of cm
Weight	Assessed at surgery	in units of Kg
Body mass index (BMI)	Defined as the body mass divided by the square of the body height	in units of Kg/m2
Body surface area (BSA)	Assessed according to the method as proposed by Haycock et al [2] Weight $[kg]^{0.5378} \times$ Height $[cm]^{0.3964} \times 0.024265$	in units of m2
Heart rate	Assessed at rest on the day of hospital admission	in units of bpm
Respiratory rate	Assessed at rest on the day of hospital admission	in units of bpm
Systolic blood pressure (SBP)	Assessed at rest on the day of hospital admission	in units of mm Hg
Diastolic blood pressure (DBP)	Assessed at rest on the day of hospital admission	in units of mm Hg
Blood pressure difference	Assessed at rest on the day of hospital admission = (SBP - DBP)	in units of mm Hg
Mean blood pressure (MBP)	Assessed at rest on the day of hospital admission = (SBP + 2 × DBP) /3	in units of mm Hg

Preoperative variables		
Clinical profiles		
Systemic arterial saturation	Assessed by pulse oximetry	in units of %
Hematocrit	Calculated by an automated analyzer before surgery Defined as the volume percentage (vol %) of red blood cells in blood, and determined by multiplying the red cell count by the mean cell volume.	in units of %
Cyanosis	Assessed based on the physical examination (e.g. the color of lips and tongue) taking into consideration state of the body. None: determined as the patient not acquiring a significant bluish tinge both at rest and at exercise Minor: determined as the patient acquiring a significant bluish tinge at exercise only Major: determined as the patient acquiring a significant bluish tinge even at rest.	none, minor, vs major
Tet spell history	Assessed according to the clinical signs and symptoms Absence presence	absence vs presence
Right bundle branch block (RBBB)	Assessed by routine 12-lead electrocardiogram at rest Normal incomplete right bundle branch block complete right bundle branch block	absence vs presence
NYHA classification	Assessed according to the New York Heart Association (NYHA) Functional Classification I: Cardiac disease, but no symptoms and no limitation in ordinary physical activity, e.g. no shortness of breath when walking, climbing stairs etc. II: Mild symptoms (mild shortness of breath and/or angina) and slight limitation during ordinary activity.	I-II vs III-IV

	III: Marked limitation in activity due to symptoms, even during less-than-ordinary activity, e.g. walking short distances (20–100 m); comfortable only at rest. IV: Severe limitations. Experiences symptoms even while at rest. Mostly bedbound patients.	
Cardiac assessment for infant	Assessed according to the modified Ross scoring system of congestive heart failure signs [3]. Each sign or symptom was graded on a scale of 0, 1, or 2 points according to the severity. The sum of points formed the clinical score (range, 0–12 points), with a higher total score corresponding to more severe heart failure: 0–2=no CHF; 3–6=mild CHF; 7–9=moderate CHF; 10–12=severe CHF. In keeping with NYHA class, we equate no CHF with NYHA class I, equate mild CHF with NYHA class II, equate moderate CHF with NYHA class III, and equate severe CHF with NYHA class IV.	0-6 [NYHA class I-II] vs 6-12[NYHA class III-IV]
Anatomical profiles		
Ventricular septal defect subtypes	Assessed based on their location in the ventricular septum by transthoracic echocardiography and/or radiographic examinations Infracristal Subarterial	infracristal vs subarterial
Ventricular septal defect scale	Assessed based on the ratio of defect to aortic root diameter small [<1/3], medium [1/3-2/3], large [>2/3]	small, medium, vs large
LV ejection fraction	Assessed by transthoracic echocardiography expressed in units of %%	in units of cm/m2
Indexed left atrial diameter	Assessed by transthoracic echocardiography Defined as left atrial diameter divided by BSA	in units of cm/m2

Indexed right atrial diameter	Assessed by transthoracic echocardiography Defined as right atrial diameter divided by BSA	in units of cm/m2
Indexed LV end-diastolic diameter	Assessed by transthoracic echocardiography Defined as LV end-diastolic diameter divided by BSA	in units of cm/m2
Indexed RV end-diastolic diameter	Assessed by transthoracic echocardiography Defined as RV end-diastolic diameter divided by BSA	in units of cm/m2
Indexed LV end-diastolic volume	Assessed by transthoracic echocardiography Defined as LV end-diastolic volume divided by BSA	in units of ml/m2
Ventricular septal defect subtypes	Assessed by transthoracic echocardiography as the ratio of ventricular septal defect to aorta Small (<1/3) Medium (1/3-2/3) Large (>2/3)	small vs medium vs large
Collateral circulation	Assessed based on their location in the ventricular septum by transthoracic echocardiography and/or radiographic examinations Minimal Minor Major	minimal vs minor vs major
McGoon ratio	Assessed based on their location in the ventricular septum by transthoracic echocardiography and/or radiographic examinations Defined as the sum of the diameters of the left and right pulmonary arteries, divided by the descending aorta diameter at diaphragm level. The McGoon index was determined using radiographic data before the operation. If radiographic data were unavailable, the echocardiography data were analyzed instead. ≤1.5	≤1.5 vs >1.5

	>1.5	
Interventricular shunting	Assessed by transthoracic echocardiography Predominantly left-to-right Predominantly bi-directional Predominantly right-to-left	left-to-right, bi-directional, vs right-to-left
RVOT pressure gradient	Assessed by transthoracic echocardiography Mild Moderate Severe	mild, moderate, vs severe
RVOTO level	Assessed by transthoracic echocardiography Infundibulum pulmonary valve main and/or branch arteries	Infundibulum, pulmonary valve, vs main and/or branch arteries
Aortic overriding	Assessed by transthoracic echocardiography ≤50% >50%	≤50% vs >50%
Patent ductus arteriosus (PDA)	Assessed by transthoracic echocardiography Absence presence	absence vs presence
Intraoperative signatures		
Surgical profiles		
Repair approach	Assessed according to the surgical approach used to repair VSD	transatrial/transpulmon

	Transatrial/transpulmonary Transventricular Transatrial plus transventricular	ary, transventricular, vs transatrial plus transventricular
Transannular repair	Classified according to absence or presence of transannular repair Absence Presence	absence vs presence
RVOTO repair option	Classified according to RVOT repair taking into account the available pathologic anatomy as well as surgeon's preference. Parietal muscle resection Infundibular outflow patch Valve-sparing procedure Transannular patch	parietal muscle resection, infundibular outflow patch, valve-sparing procedure, vs transannular patch
Pulmonary patch	Classified according to absence and detailed subtypes of pulmonary patch taking into account the available the degree of pulmonary stenosis as well as surgeon's preference. Absence transannular patch alone combined main patch combined branch patch	absence, transannular patch alone, combined main patch, vs combined branch patch
Tricuspid valve detachment	Classified according to whether it involves tricuspid valve detachment Absence Presence	absence vs presence
Extracorporeal profiles		
Cannulation approach	Classified according to cannulation approach for CPB taking into account the patient's weight and cardiovascular anatomy as well as surgeon's preference.	bicaval venous vs RAA-venous

	Aorto-superior and inferior vena cava cannulation Aorto- inferior vena cava and right atrial appendage cannulation	
Reoxygenation level	Assessed during the aortic cross clamp by arterial blood gas analysis Lower [≤250 mm Hg] Higher [>250 mmHg]	lower vs higher
Cardioplegia solution	Following the aortic cross clamp, cold blood cardioplegic solution was antegrade perfused for myocardial preservation at an initial dose of 20 ml/kg and a maintenance dose of 10 ml/kg at a temperature of 4°C -8°C. Buckberg cardioplegia (4:1 blood cardioplegia solution) del Nido Cardioplegia (1:4 blood cardioplegia solution) HTK cardioplegia (histidine-tryptophan-ketoglutarate cardioplegia)	Buckberg, del Nido vs HTK
CPB hypothermia	Classified according to complete repair under the temperature on bypass Mild hypothermia Moderate hypothermia	mild vs moderate
CPB duration	Calculated between the starting of cannulation and weaning from bypass	in units of min

LV=left ventricle; RV=right ventricle; RVOTO=right ventricular outflow tract obstruction; CPB= cardiopulmonary bypass.

Reference

[1] Goldstein B, Giroir B, Randolph A. International pediatric sepsis consensus conference: Definitions for sepsis and organ dysfunction in pediatrics. Pediatr Crit Care Med, 2005, 6(1):2-8.

[2] Haycock GB, Schwartz GJ, Wisotsky DH. Geometric method for measuring body surface area: A height-weight formula validated in infants, children, and adults. J Pediatr 1978;93:62-6.

[3] Ross RD, Bollinger RO, Pinsky WW. Grading the severity of congestive heart failure in infants. Pediatr Cardiol 1992; 13: 72–75

Table S2. Baseline and perioperative characteristics of patients in derivation cohort used for nomogram construction: pre-imputation and post-imputation.

Variables	Derivation cohort (N=513)		
	pre-imputation	post-imputation	P value
Continuous variables			
Age at surgery, month	30.7 (13.5- 60.8)	30.7 (13.5- 60.8)	
Height, cm	85.0 (74.0-102.0)	85.0 (74.0-102.0)	
Weight, kg	11.4 (9.0- 15.4)	11.4 (9.0- 15.4)	
Body mass index, kg/m^2	15.62 (14.18- 17.09)	15.62 (14.18- 17.09)	
Heart rate, bpm	118 (106-132)	118 (106-132)	
Respiratory rate, bpm	25 (22- 27)	25 (22- 27)	
Systolic blood pressure, mm Hg	97 (92-105)	97 (92-105)	
Diastolic blood pressure, mm Hg	57 (52- 64)	57 (52- 64)	
Blood pressure difference, mm Hg	40 (35- 46)	40 (35- 46)	
Mean blood pressure, mm Hg	70.3 (65.3- 77.7)	70.3 (65.3- 77.7)	
Age group at surgery, %			
Infant (1mon-1yr)	216 (42.1%)	216 (42.1%)	
Toddler and preschool (2-5 yrs)	190 (37.0%)	190 (37.0%)	
School age child (6-12 yrs)	92 (17.9%)	92 (17.9%)	
Adolescent (13-18 yrs)	15 (2.9%)	15 (2.9%)	
Systemic arterial saturation, %	83 (77- 93)	83 (77- 93)	
Hematocrit, %	43.6 (38.1- 50.5)	43.6 (38.1- 50.5)	
Indexed LVEDV, ml/m^2	26.5 (20.8- 33.7)	27.1 (20.7- 35.7)	0.387
Missing	193 (37.6%)		
Indexed LVEDD, mm/m^2	44.59 (38.0- 52.1)	45.53 (38.2- 53.5)	0.348
Missing	152 (29.6%)		
Indexed LA diameter, mm/m^2	36.0 (30.6- 41.4)	36.1 (30.3- 42.2)	0.348
Missing	153 (29.8%)		
Indexed RVEDD, mm/m^2	48.3 (41.0- 53.9)	48.4 (40.6- 54.4)	0.795
Missing	156 (30.4%)		
Indexed RA diameter, mm/m^2	49.7 (41.8- 56.1)	49.7 (40.9- 56.2)	0.751
Missing	156 (30.4%)		
LV ejection fraction, %	62 (60- 65)	63 (60- 66)	0.982
Missing	157 (30.6%)		
CPB duration, min	121 (90-155)	121 (90-156)	0.800
Missing	7 (1.4%)		
Categorical variables, %			

Sex			
Female	221 (43.1%)	221 (43.1%)	
Male	292 (56.9%)	292 (56.9%)	
Cyanosis degree			
None	137 (26.7%)	137 (26.7%)	
Minor	174 (33.9%)	174 (33.9%)	
Major	202 (39.4%)	202 (39.4%)	
NYHA class			
I-II	479 (93.4%)	479 (93.4%)	
III-IV	34 (6.6%)	34 (6.6%)	
Right bundle branch block			
Absence	463 (90.3%)	463 (90.3%)	
Presence	50 (9.8%)	50 (9.8%)	
Interventricular shunting			
Predominantly left-to-right	58 (11.3%)	58 (11.3%)	
Predominantly bi-directional	432 (84.2%)	432 (84.2%)	
Predominantly right-to-left	23 (4.5%)	23 (4.5%)	
Overriding aorta			
≤50%	438 (85.4%)	438 (85.4%)	
>50%	75 (14.6%)	75 (14.6%)	
Cannulation approach			
RA-venous	431 (84.2%)	431 (84.2%)	
bicaval venous	82 (15.8%)	82 (15.8%)	
RVOT pressure gradient			
Mild	163 (31.8%)	163 (31.8%)	
Moderate	181 (35.3%)	181 (35.3%)	
Severe	169 (32.9%)	169 (32.9%)	
Ventricular septal defect subtypes			
Infracristal	456 (88.9%)	456 (88.9%)	
Subarterial	57 (11.1%)	57 (11.1%)	
Collateral arteries			
Minimal	383 (74.7%)	383 (74.7%)	
Minor	73 (14.2%)	73 (14.2%)	
Major	57 (11.1%)	57 (11.1%)	
Patent ductus arteriosus			
Absence	373 (72.7%)	373 (72.7%)	
Presence	140 (27.29%)	140 (27.29%)	

RVOTO level			
Infundibulum	229 (44.6%)	229 (44.6%)	
Pulmonary valve	55 (10.7%)	55 (10.7%)	
Main and/or branch arteries	229 (44.6%)	229 (44.6%)	
Repair approach			
Transatrial-transpulmonary	249 (48.5%)	249 (48.5%)	
Transventricular	236 (46.0%)	236 (46.0%)	
Transatrial plus transventricular	28 (5.5%)	28 (5.5%)	
Transannular patch			
Absence	229 (44.6%)	229 (44.6%)	
Presence	284 (55.4%)	284 (55.4%)	
RVOTO repair option			
Parietal muscle resection	23 (4.5%)	23 (4.5%)	
Infundibular outflow patch	76 (14.8%)	76 (14.8%)	
Valve-sparing	130 (25.3%)	130 (25.3%)	
Transannular patch	284 (55.4%)	284 (55.4%)	
Pulmonary patch			
Absence	229 (44.6%)	229 (44.6%)	
Transannular patch alone	55 (10.7%)	55 (10.7%)	
Combined main patch	190 (37.0%)	190 (37.0%)	
Combined branch patch	39 (7.6%)	39 (7.6%)	
Tricuspid valve detachment			
Absence	409 (79.7%)	409 (79.7%)	
Presence	104 (20.3%)	104 (20.3%)	
Cardioplegia solution			
Standard Buckberg protocol	168 (32.8%)	168 (32.8%)	
del Nido protocol	345 (67.3%)	345 (67.3%)	
HTK protocol	0 (0%)	0 (0%)	
Tet spell history			0.953
Absence	298 (58.7%)	300 (58.5%)	
Presence	210 (41.3%)	213 (41.5%)	
Missing	5 (1.0%)		
McGoon index			0.459
>1.5	264 (66.5%)	353 (68.8%)	
≤1.5	133 (33.5%)	160 (31.2%)	
Missing	116 (22.6%)		
Ventricular septal defect scale			0.999

Small	176 (34.4%)	177 (34.5%)	
Medium	171 (33.4%)	171 (33.3%)	
Large	165 (32.2%)	165 (32.2%)	
Missing	1 (0.2%)		
CPB Hypothermia scale			0.931
Mild	192 (37.9%)	196 (38.2%)	
Moderate	314 (62.1%)	317 (61.8%)	
Missing	7 (1.4%)		
Reoxygenation level			
Lower	225 (43.9%)	225 (43.9%)	
Higher	288 (56.1%)	288 (56.1%)	
Missing	0		

Continuous data are presented as median (IQR) and dichotomous data are presented as counts (%).

LVEDV= left ventricle end-diastolic volume; LVEDD=left ventricle end-diastolic diameter; RVEDD=right ventricle end-diastolic diameter; LA=left atrial; RA=right atrial; RVOTO=right ventricular outflow tract obstruction; CPB= cardiopulmonary bypass.

Table S3. Selected baseline and perioperative characteristics of patients in validation cohort used for nomogram validation: pre-imputation and post-imputation.

Variables	Validation cohort (N=158)		
	pre-imputation	post-imputation	P value
Baseline variables			
Age at surgery, months	28.7 (13.4-55.1)	28.7 (13.4- 55.1)	1.000
Missing	0		
Age group at surgery, (%)			1.000
Infant (1mon-1yr)	66 (41.8%)	66 (41.8%)	
Toddler and preschool (2-5 yrs)	64 (40.5%)	64 (40.5%)	
School age child (6-12 yrs)	21 (13.3%)	21 (13.3%)	
Adolescent (13-18 yrs)	7 (4.4%)	7 (4.4%)	
Missing	0		
Mean blood pressure, mm Hg	46.8 (42.1- 49.3)	46.8 (42.1- 49.3)	1.000
Missing	0		
Preoperative variables			
Hematocrit, %	43.2 (38.1- 49.4)	43.2 (38.1- 49.5)	0.991
Missing	2 (1.27%)		
Indexed LVEDV, ml/m^2	27.3 (21.6-38.8)	27.5 (21.9- 37.3)	0.842
Missing	50 (31.7%)		
Indexed RA diameter, mm/m^2	49.7 (43.4- 57.8)	49.1 (39.5- 55.6)	0.344
Missing	43 (27.2%)		
Cyanosis degree, (%)			0.997
None	45 (28.7%)	45 (28.5%)	
Minor	53 (33.8%)	53 (33.5%)	
Major	59 (37.6%)	60 (38.0%)	
Missing	1 (0.63%)		
Tet spell history, (%)			0.962
Absence	92 (58.6%)	93 (58.9%)	
Presence	65 (41.4%)	65 (41.1%)	
Missing	1 (0.6%)		
NYHA functional class, (%)			0.990
I-II	149 (94.9%)	150 (94.94%)	
III-IV	8 (5.1%)	8 (5.1%)	
Missing	1 (0.63%)		
Right bundle branch block, (%)			0.973
Absence	143 (91.7%)	145 (91.8%)	

Presence	13 (8.3%)	13 (8.2%)	
Missing	2 (1.27%)		
Interventricular shunting, (%)			0.999
Predominantly left-to-right	17 (10.9%)	17 (10.7%)	
Predominantly bi-directional	130 (83.3%)	132 (83.5%)	
Predominantly right-to-left	9 (5.8%)	9 (5.7%)	
Missing	2 (1.3%)		
Aortic overriding, (%)			0.889
≤50%	139 (89.1%)	140 (88.6%)	
>50%	17 (10.9%)	18 (11.4%)	
Missing	2 (1.3%)		
McGoon index, (%)			0.881
>1.5	103 (71.0%)	111 (70.3%)	
≤1.5	42 (29.0%)	47 (29.8%)	
Missing	13 (8.2%)		
Collateral arteries, (%)			0.999
Minimal	108 (68.8%)	109 (69.0%)	
Minor	27 (17.2%)	27 (17.1%)	
Major	22 (14.0%)	22 (13.9%)	
Missing	1 (0.6%)		
Intraoperative variables			
Reoxygenation level, (%)			0.926
Lower (≤ 250 mmHg)	63 (59.4%)	93 (58.9%)	
Higher (>250 mmHg)	43 (40.6%)	65 (41.1%)	
Missing	52 (32.9%)		
Tricuspid valve detachment, (%)			1.000
Absence	127 (80.4%)	127 (80.4%)	
Presence	31 (19.6%)	31 (19.6%)	
Missing	0		
RVOTO repair, (%)			1.000
Parietal muscle resection	8 (5.1%)	8 (5.1%)	
Infundibular outflow patch	19 (12.0%)	19 (12.0%)	
Valve-sparing repair	43 (27.2%)	43 (27.2%)	
Transannular patch	88 (55.7%)	88 (55.7%)	
Missing	0		
CPB duration, min	121 (95-152)	122 (95-154)	0.924
Missing	1 (0.6%)		

Continuous data are presented as median (IQR) and dichotomous data are presented as counts (%). LVEDV=left ventricle end-diastolic volume; RA=right atrial; RVOTO=right ventricular outflow tract obstruction; CPB= cardiopulmonary bypass; post-LCOS: postoperative low cardiac output syndrome.

Table S4. Comparison of multiple rates for each risk group.

	Total patients	Patients with In-hospital Complications	Patients without In-hospital Complications	Dunnett's modified test level α'	Crude P value
Triple risk categories, n					
Low risk group	242	13	229	0.05/(3-1)=0.025	-
Intermediate risk group	137	18	119	0.05/(3-1)=0.025	0.008*
High risk group	134	45	89	0.05/(3-1)=0.025	<0.001*
ARIAR-Risk categories, n					
Absolute low risk group	68	1	67	0.05/(5-1)=0.0125	-
Relative low risk group	174	12	162	0.05/(5-1)=0.0125	0.092#
Intermediate risk group	137	18	119	0.05/(5-1)=0.0125	0.005#
Aggressive high risk group	108	31	77	0.05/(5-1)=0.0125	<0.001#
Refractory high risk group	26	14	12	0.05/(5-1)=0.0125	<0.001#

*Compared with low risk group (as control).

#Compared with absolute low risk group (as control).

Figure S1. Flow charts of the derivation (A) and validation (B) cohort.

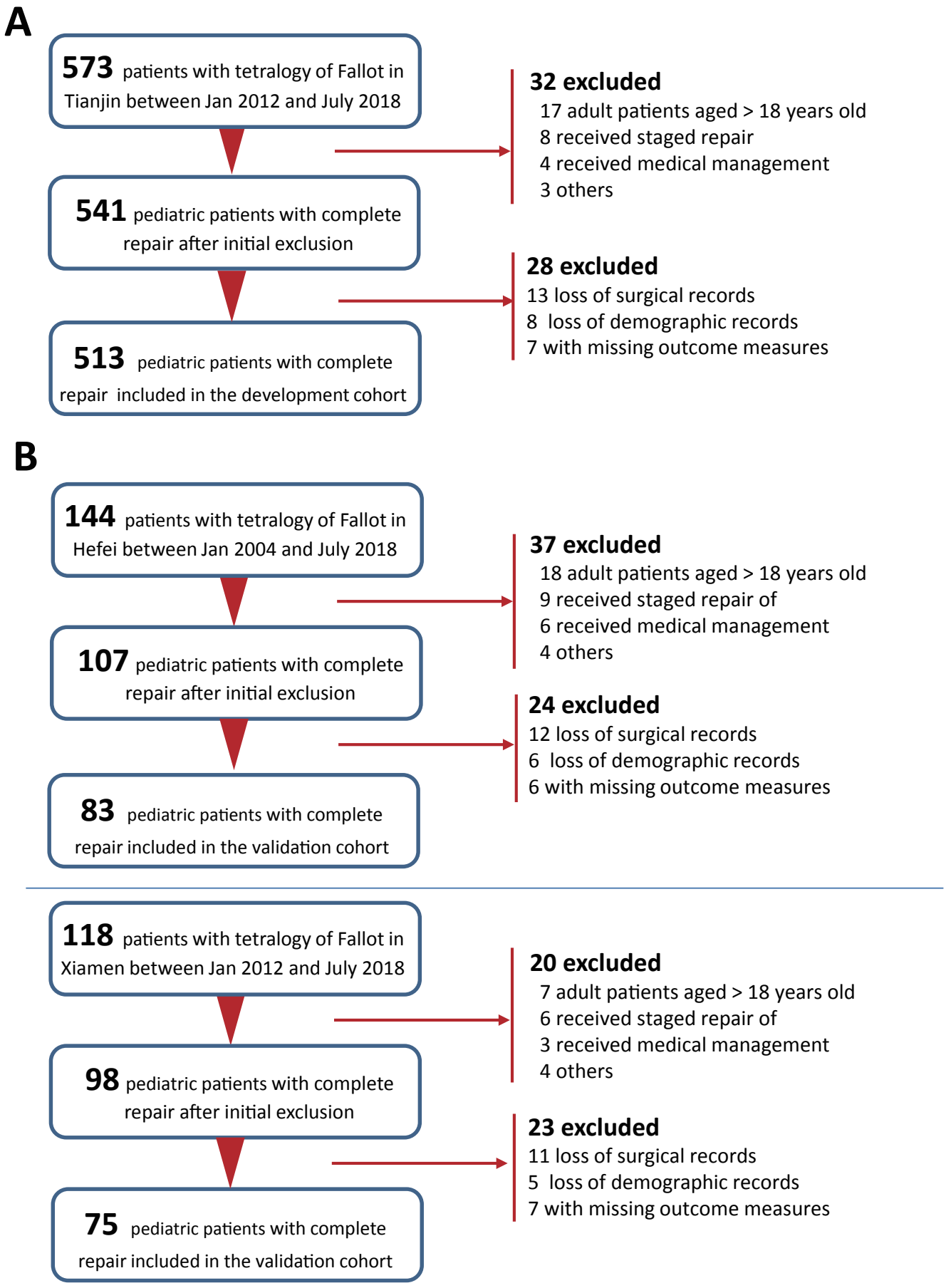

Figure S2.

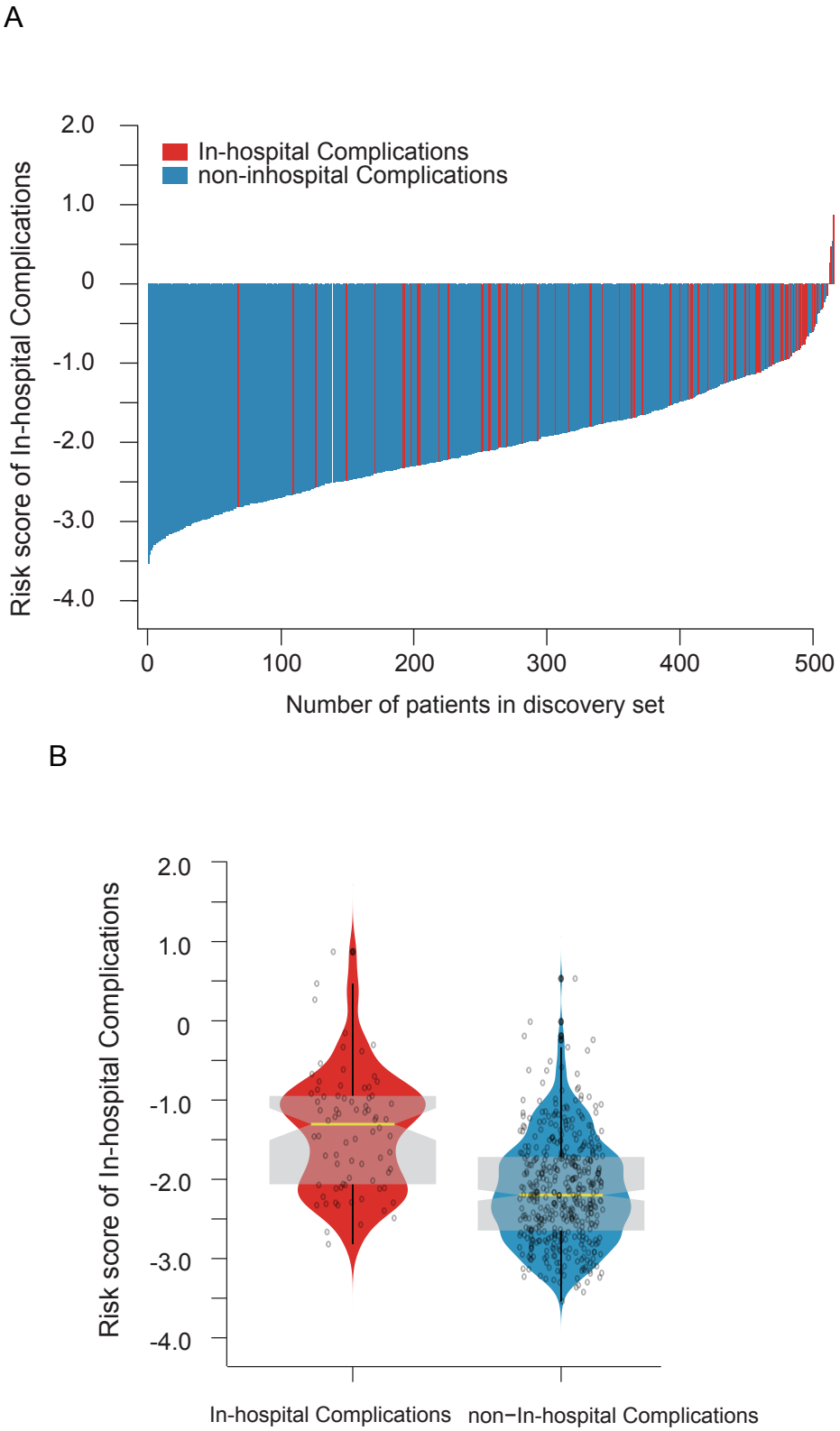

(A) The distribution plots of risk score of in-hospital complications among derivation cohort
(B) Violin plots for risk score of in-hospital complications in patients with or without in-hospital complications. The width of the colored shape indicates the probability density of patients with a given result. The gray notched box plots represent the median (yellow horizontal line), 95% confidence interval of the median (notch), interquartile range (25th to 75th percentile) (box), and the upper 1.5 times the interquartile range (solid vertical line).

Figure S3. Association between risk-based classifier and risk of in-hospital complications.

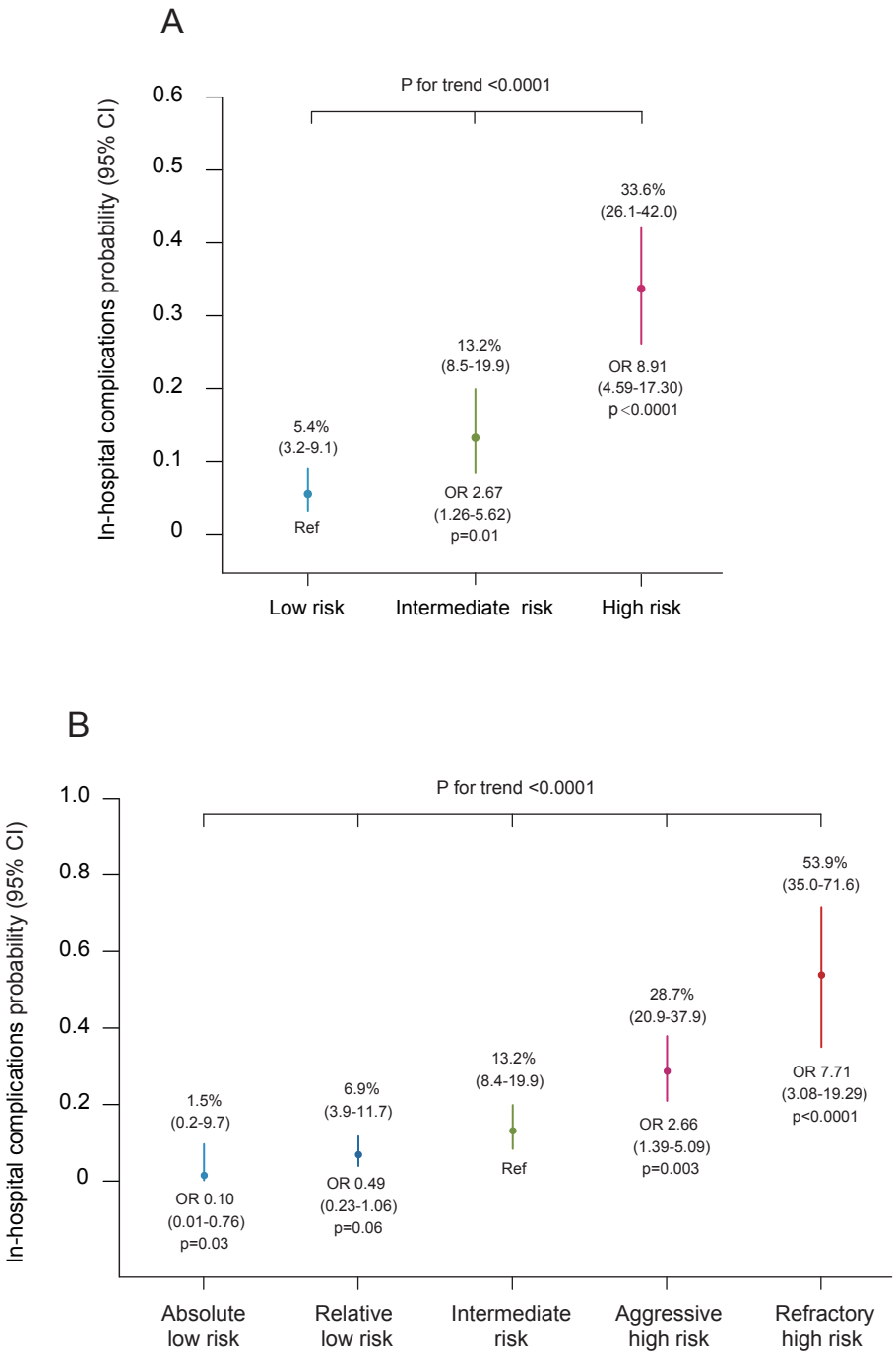

Unadjusted association between triple risk classifier (A) and ARIAR-risk classifier (B) and probability and odd ratio (OR) of in-hospital complications with 95% confidence intervals (CI).

Figure S4. Distribution of selected variables according to year of surgery.

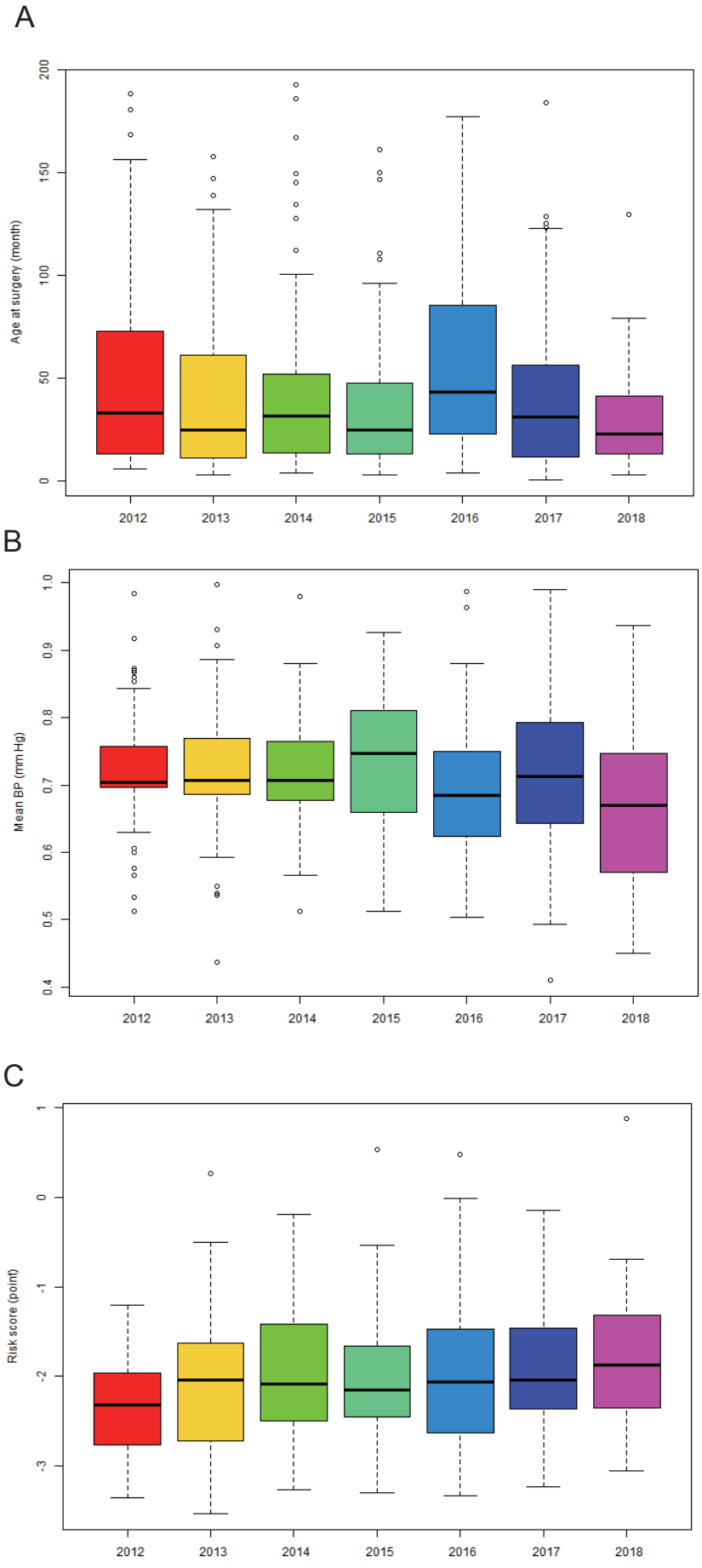

Patient's age at surgery (A), mean BP (B), and risk score (C) according to year of surgery in derivation cohort
Data are presented as medians with Tukey's whiskers (boxes represent IQRs and bars represent 50% extreme quartiles).
BP=blood pressure.